

Resource Assessment of Wind Energy Potential of Mokha in Yemen with Weibull Speed

Abdulbaset El-Bshah¹, Fahd N. Al-Wesabi^{2,3,*}, Ameen M. Al-Kustoban⁴, Mohammad Alamgeer⁵,
Nadhem Nemri⁵, Majdy M. Eltahir⁵, Hany Mahgoub⁶ and Noha Negm⁷

¹Department of Electronic Engineering, Faculty of Engineering, University of Science and Technology UST-Sana'a, Yemen

²Department of Computer Science, King Khalid University, Muhayel Aseer, Kingdom of Saudi Arabia

³Faculty of Computer and IT, Sana'a University, Sana'a, Yemen

⁴Department of Electronic, Faculty of Engineering, UST, Sana'a, Yemen

⁵Department of Information Systems, King Khalid University, Mayahel Aseer, KSA

⁶Department of Computer Science, King Khaled University, KSA & Faculty of Computers and Information,
Menoufia University, Egypt

⁷Department of Computer Science, King Khaled University, KSA & Faculty of Science, Department of Mathematics and
Computer Science, Menoufia University, Egypt

*Corresponding Author: Fahd N. Al-Wesabi. Email: falwesabi@kku.edu.sa

Received: 07 March 2021; Accepted: 08 April 2021

Abstract: The increasing use of fossil fuels has a significant impact on the environment and ecosystem, which increases the rate of pollution. Given the high potential of renewable energy sources in Yemen and other Arabic countries, and the absence of similar studies in the region. This study aims to examine the potential of wind energy in Mokha region. This was done by analyzing and evaluating wind properties, determining available energy density, calculating wind energy extracted at different altitudes, and then computing the capacity factor for a few wind turbines and determining the best. Weibull speed was verified as the closest to the average actual wind speed using the cube root, as this was verified using 3 criteria for performance analysis methods ($R^2 = 0.9984$, $RMSE = 0.0632$, $COE = 1.028$). The wind rose scheme was used to determine the appropriate direction for directing the wind turbines, the southerly direction was appropriate, as the winds blow from this direction for 227 days per year, and the average southerly wind velocity is 5.27 m/s at an altitude of 3 m. The turbine selected in this study has a tower height of 100m and a rated power of 3.45 MW. The capacitance factor was calculated for the three classes of wind turbines classified by the International Electrotechnical Commission (IEC) and compared, and the turbine of the first class was approved, and it is suitable for the study site, as it resists storms more than others. The daily and annual capacity of a single, first-class turbine has been assessed to meet the needs of 1,447 housing units in Mokha region.



This work is licensed under a Creative Commons Attribution 4.0 International License, which permits unrestricted use, distribution, and reproduction in any medium, provided the original work is properly cited.

The amount of energy that could be supplied to each dwelling was around 19 kWh per day, which was adequate to power the basic loads in the home.

Keywords: Wind energy system; probability density; wind speed; Weibull velocity; Rayleigh velocity; wind rose

1 Introduction

The increase in population and rate of industrialization has led to a rise in energy demand. Fossil fuels cannot meet this demand because they negatively affect the environment and ecosystem, causing a significant increase in pollution. In other words, the energy industry and the environment are in significant crises today. Today in modern societies, energy is the most important indicator of economic growth and many countries worldwide are taking steps toward achieving a renewable energy model to solve this crisis [1,2]. Renewable energy sources such as solar, thermal, geothermal, bioenergy, hydropower, and ocean have gained popularity all over the world due to their distinct characteristics. Simultaneously, the increasing use of fossil fuels and the resulting environmental pollution has motivated researchers to find other sustainable, clean, efficient, and economical energy sources. Wind power systems are known to operate on a wind speed system. In 2800 BC, wind energy was used to pump water and generate power in rural areas. Wind energy is used today as an alternative source of energy [3,4].

As seen in literature [5–9] and in various places around the world, great emphasis has been placed on the Weibull function because it is suitable for wind speed data analysis. It is also useful for distributing large statistical data and is presented as a continuous distribution for further analysis. Some literature [10–18] are related to renewable energy in the Republic of Yemen, despite the scarcity of that literature due to a similar study for this region. Geographically, Yemen is located between latitude 13 north and 16 norths and longitude 43.2–53.2 in southwestern Asia. The Red Sea surrounds it from the west and the Indian Ocean (Arabian Sea) from the south. The total area of Yemen is 527,970 km², and as of 2016, the population was about 26,687,000 people. Yemen has a high potential for renewable energy sources such as solar, wind, and geothermal energy [19–21].

In 2009, the Yemeni government approved the National Renewable Energy and Efficiency Strategy, which aims to increase 15% of energy efficiency (EE) in the energy sector by 2025, and target renewable energy (RE) capacity (Geothermal energy 160 megawatts, concentrated solar power 100 megawatts, solid biomass 6 megawatts, solar photovoltaic system 8.25, and wind power 400 megawatts) of total electricity by 2025. The Yemeni energy sector consists of oil, natural gas, and biofuel production. Energy production in 2012 was “15.109 kilotons of oil equivalent (ktoe), while consumption was 6,923 kilotons” [22–24].

The objective of this study is divided into three parts are: to find a probability distribution function that gives the best estimate of annual wind energy and is close to the actual value of this energy. Using the wind rose chart, the prevailing wind direction during the seasons of the year is determined at the study site. Study the characteristics of the three classes of wind turbines, calculate the capacitance factor for each of them, and determine the most appropriate class for the study site.

The rest of the paper has four more sections. Section 2 provides the methodology. Section 3 provides the basic calculations of the proposed system model. Section 4 presents the results and discussion, and Section 5 offers conclusions.

2 Methodology

The research consists of two main parts, and each section consists of its own parts. In the first section, the statistical analysis of the measured wind speed data from the OYMK monitoring station was performed at a height of 3 m in the MOKHA area for five years (2011 to 2015), and these speeds will be converted to be suitable for wind turbine heights of 30 and 100 m.

Since the statistical values of wind speed measurements do not express the power that can be derived from these measured speeds, so the probability distribution functions that help us in evaluating wind energy from the statistical values of wind speed will be used only (without knowing the measured values).

To demonstrate the accuracy of the work of these functions, the cubic statistical values of wind speeds will be calculated and the actual power values compared to the power evaluated by the probability distribution functions, where the most used functions for the probability distribution of the wind speed measured at a given location are the Weibull and Rayleigh distributions.

In the second section, power factors for the three popular classes of rated wind turbines according to the International Electrotechnical Commission (IEC) were calculated, and the wind rose analysis was made in order to determine the most appropriate direction for steering the turbine. Also, in this section, the amount of energy that can be harvested during the year with one turbine with a rated capacity of 3450 kilowatts will be calculated, and the amount of energy required to meet the needs of Mokha region will be determined.

3 Basic Calculations of the Proposed System Model

3.1 Wind Measurement Site

The Mokha region is located at longitude $43^{\circ}16'60'$ east and latitude $13^{\circ}19'0'$ north. It overlooks the Red Sea in southwestern Yemen and is 75 km north of Bab al-Mandab, 100 km west. The city of Taiz, and 170 km south of Hodeidah. The OYMK monitoring station is located 8 km south of Mokha, at a longitude $43^{\circ}16'60''$ east and $13^{\circ}15'00''$ north latitude, at a height of 3 m from the ground. The location of the OYMK monitoring station and the distance between it and Mocha. [Tab. 1](#) shows the most recent observation of this city, while [Tab. 2](#) shows the administrative division of this city, where we note in order to provide a wind power generation system for 1447 houses, comprising 1452 households with 10428 residents. [Tab. 1](#) show the most recent observation for Mokha.

Table 1: The most recent observation for Mokha region

Observation	Value
Air temperature [F]	80.6
Maximum air temperature [F]	80.6
Minimum air temperature [F]	77
Dew point [F]	69.8
Wind direction	S (180 degrees)
Wind speed [m/s] at h = 10 m	9.3 m/s

Table 2: The statistical values of wind speed measured by OYMK station at h= 3m

Year	2011		2012		2013		2014		2015		Yearly		Sector 30° direction
	\bar{v}	σ	\bar{v}	σ	\bar{v}	σ	\bar{v}	σ	\bar{v}	σ	\bar{v}	σ	
Jan	–	–	4.73	2.21	5.65	1.99	6.12	1.53	4.32	2.43	5.17	2.20	S
Feb	–	–	6.01	2.22	6.03	2.02	5.23	2.17	7.68	3.88	6.24	2.83	S
Mar	–	–	5.03	2.10	5.51	1.87	6.90	2.46	7.51	0.89	6.05	2.23	S
Apr	–	–	5.10	2.02	3.87	1.44	5.84	1.97	–	–	4.87	1.99	S
May	–	–	4.15	1.54	3.53	1.57	3.41	1.64	–	–	3.71	1.62	S
Jun	–	–	1.74	0.97	2.01	0.85	2.73	2.19	–	–	2.18	1.53	N/NW
Jul	–	–	1.80	1.07	2.11	1.32	2.58	1.39	–	–	2.16	1.31	N/NW
Aug	2.45	0.41	2.14	1.25	1.75	1.57	1.89	1.12	–	–	1.98	1.29	N/NW
Sep	2.60	1.03	2.87	1.36	2.53	1.01	1.81	0.63	–	–	2.45	1.11	N/NW
Oct	4.37	1.62	5.18	1.20	3.57	1.89	2.83	1.36	–	–	4.00	1.77	S
Nov	3.99	1.83	5.44	1.08	5.99	1.12	3.82	0.99	–	–	4.85	1.60	S
Dec	5.09	1.87	4.87	1.21	5.14	1.98	4.56	1.43	–	–	4.97	1.71	S
Annual	3.92	1.84	4.12	2.16	3.89	2.22	3.92	2.37	6.25	3.29	4.11	2.35	

3.2 Data Collection and Validation

In this study, environmental data available on the Iowa Environmental Mesonet (IEM) was analyzed. IEM collects environmental data from cooperating members with observing networks. The data are stored and made available on the website [24].

The data analyzed are wind data extracted from the integrated surface database (ISD) of the OYMK monitoring station, and the data block consisted of 16315 wind speed measurements on an hourly head (between August 23, 2011 and March 18, 2015), and the largest measured value was wind speed It is 92 m/s while the lowest value is 0.52 m/s, and the temperature ranged between 0° and 380. We note also that the data for the years 2011 and 2015 are incomplete.

In order to simplify the analysis, these data were summarized by calculating the average value for each day and we reduced the data block to 1,221 average daily wind speed.

3.3 Estimation of Weibull-Rayleigh Parameters

The probability density function of a Weibull distribution can be expressed as given in Eq. (1).

$$f_w(v) = \left(\frac{k}{c}\right) \left(\frac{v}{c}\right)^{k-1} \exp\left[-\left(\frac{v}{c}\right)^k\right] \quad (1)$$

The cumulative distribution function of a Weibull distribution is expressed by the integration of the probability density function as given in Eq. (2).

$$F_w(v) = 1 - \exp\left[-\left(\frac{v}{c}\right)^k\right] \quad (2)$$

As the two parameters of the Weibull distribution are shape factor k and scale factor c , which can be related to mean wind speed \bar{v} and standard deviation σ by Eqs. (3) and (4).

$$k = \left(\frac{\sigma}{\bar{v}}\right)^{-1.086} \quad (3)$$

$$c = \left(\frac{\bar{v}}{\Gamma\left(1 + \frac{1}{k}\right)}\right) \quad (4)$$

The Rayleigh distribution is a special case of a Weibull distribution with the shape parameter value of the constant $k = 2$, where the probability distribution and the cumulative distribution are determined by Eqs. (5)–(7) below.

$$f_R(v) = \frac{2v}{c_R^2} \exp\left[-\left(\frac{v}{c_R}\right)^k\right] \quad (5)$$

$$F_R(v) = 1 - \exp\left[-\left(\frac{v}{c_R}\right)^k\right] \quad (6)$$

$$c_R = \frac{2\bar{v}}{\sqrt{\pi}} \quad (7)$$

The mean value of wind speed \bar{v} and standard deviation σ in terms of the parameter of Weibull k and c are determined as follows, where $\Gamma(\cdot)$ is the gamma function as shown in Eqs. (8) and (9).

$$\bar{v} = c\Gamma\left(1 + \frac{1}{k}\right) \quad (8)$$

$$\sigma = c\left[\Gamma\left(1 + \frac{2}{k}\right) - \Gamma^2\left(1 + \frac{1}{k}\right)\right]^{\frac{1}{2}} \quad (9)$$

Sometimes two wind amplitudes should be taken seriously to assess the wind energy potential of a site, namely the most probable wind speed v_{wmp} and the wind speed carrying the maximum energy v_{wEm} , and these are expressed in terms of the Weibull and Rayleigh parameters as given in Eqs. (10)–(13) below.

$$v_{wmp} = c\left[\frac{k-1}{k}\right]^{1/k} \quad (10)$$

$$v_{wEm} = c\left[\frac{k+2}{k}\right]^{1/k} \quad (11)$$

$$v_{Rmp} = \frac{c_R}{\sqrt{2}} = \sqrt{\frac{2}{\pi}}\bar{v} \quad (12)$$

$$v_{REm} = \sqrt{2}c_R = 2v_{Rpm} = 2\sqrt{\frac{2}{\pi}}\bar{v} \quad (13)$$

3.4 Means and Deviations

The arithmetic statistics express the mean value and the standard deviation of the wind speed measured as given by Eq. (14).

$$\bar{v} = \frac{\sum_{j=1}^N f_j \cdot v_j}{\sum_{j=1}^N f_j} \quad \sigma = \left[\frac{\sum_{j=1}^N f_j (v_j - \bar{v})^2}{\sum_{j=1}^N f_j} \right]^{\frac{1}{2}} \quad (14)$$

However, because the energy extracted from the wind is proportional to the cube of the wind speed and not with the speed itself, it is better to use cubic statistics. Cubic statistics express the mean value and standard deviation of a cube of wind speed measured as given by Eq. (15).

$$\bar{v}_{Cub} = \left(\frac{\sum_{j=1}^N f_j \cdot v_j^3}{\sum_{j=1}^N f_j} \right)^{\frac{1}{3}} \quad \sigma_{Cub} = \left[\frac{\sum_{j=1}^N f_j (v_j - \bar{v}_{Cub})^2}{\sum_{j=1}^N f_j} \right]^{\frac{1}{2}} \quad (15)$$

where \bar{v} (m/s) the average wind speed is measured, \bar{v}_{Cub} (m/s) is the cube root of average cubed wind speed is measured, v (m/s) is the actual wind speed, and N is the number of wind speeds recorded.

3.5 Performance Analysis

In order to determine the performance of the Weibull and Rayleigh models a quantitative evaluation of the performance of these models must be made. There are different methods of evaluation are Coefficient of determination, Root mean square error (RMSE), and Coefficient of efficiency (COE).

3.5.1 Coefficient of Determination (R^2)

R^2 checks the ability of the probability distribution function to accurately estimate variables. It is considered that the higher R^2 , the better the function. R^2 ranges from (0, 1) as given by Eq. (16).

$$R^2 = 1 - \frac{\sum_{j=1}^N (\hat{v}_j - v_j)^2}{\sum_{j=1}^N (v_j - \bar{v})^2} \quad (16)$$

3.5.2 Root Mean Square Error (RMSE)

RMSE verifies the accuracy of the model by checking the value obtained by the probability distribution function and the raw data measured. The lower the RMSE, the better the probability distribution function. RMSE ranges from (0, 1). RMSE will never have a negative value. RMSE is calculated using Eq. (17).

$$RMSE = \sqrt{\frac{\sum_{j=1}^N (\hat{v}_j - v_j)^2}{N}} \quad (17)$$

3.5.3 Coefficient of Efficiency (COE)

Another way to check the efficiency of a probability distribution function is to use the Coefficient of efficiency COE. The closer the value of COE to the value of the integer one, the better the accuracy of the efficiency of the probability distribution function, COE is calculated using Eq. (18).

$$\text{COE} = \frac{\sum_{j=1}^N (\hat{v}_j - \bar{v})^2}{\sum_{j=1}^N (v_j - \bar{v})^2} \quad (18)$$

where \hat{v}_j the wind speed predicted by the probability distribution function, v_j the actual measured wind speed, \bar{v} the mean value of the wind speed, N is the number of values in the data block being processed.

3.6 Wind Power Density

Power density assessment is of primary importance in assessing wind energy in a given region. The density of wind power depends on the density of the air ρ , the cube of the wind speed \bar{v}_{Cub}^3 , and the wind speed distribution f_j . Therefore, this parameter is generally considered to be a better indicator of wind resource than wind speed as given by Eq. (19).

$$\text{Actual power } P_{DCub} = 0.5\rho\bar{v}_{Cub}^3 \quad \bar{v}_{Cub} = \left[\frac{\sum_{j=1}^N f_j \cdot v_j^3}{\sum_{j=1}^N f_j} \right]^{\frac{1}{3}} \quad (19)$$

The power density can also be evaluated using the probability distribution functions as given by Eqs. (20) and (21), which help us to do so by knowing the mathematical statistics of wind speed without referring to the measured wind speeds, as we will notice in the results section.

$$\text{Weibull evaluated power } P_{Dw} = \frac{1}{2}\rho\bar{v}_w^3 \quad \bar{v}_w = \sqrt[3]{\Gamma\left(1 + \frac{3}{k}\right)} \times c \quad (20)$$

$$\text{Rayleigh evaluated power } P_{DR} = \frac{1}{2}\rho\bar{v}_R^3 \quad \bar{v}_R = 1.24 \times \bar{v} \quad (21)$$

Where \bar{v}_w and \bar{v}_R are the wind speed evaluated by the Weibull and Rayleigh distribution respectively which gives a power density close to the actual power density. The standard air density $\rho = 1.225 \text{ kg/m}^3$ dry air at 1 atm and 1.5 C°.

3.7 Extrapolation of Wind Speed at Different Axis Height

The observed data used in this study were measured at a height of 3 m. whereas most trade wind turbines have different hub heights ranging from 30 m to more than 100 m. Hence, Hillman's exponential law was used to extrapolate the wind speed data to the appropriate height for our study (100 m) as shown in Eq. (22).

$$v_2 = v_1 \left(\frac{z_2}{z_1} \right)^\alpha \quad (22)$$

where v_1 is the wind speed at height z_1 , v_2 is the wind speed at height z_2 , and α is the coefficient of friction that depends on the roughness of the surface and the stability of the atmosphere.

The monthly energy index values for all sites are generally in the Mokha region less than $\alpha = 0.19$.

Estimation of Capacity Factor (CF)

The capacity factor is an important parameter for selecting a suitable wind turbine for the studied site, and is defined as the ratio of the average power output $P_{w,avg}$ to the rated power output P_r according to the Eq. (23).

$$CF = \frac{P_{w,avg}}{P_r} \quad (23)$$

The capacitance factor can also be calculated by Eq. (24).

$$CF = \frac{1}{V_r^3} \int_{V_c}^{V_r} v^3 f(v) .dv + \int_{V_r}^{V_f} f(v) .dv \quad (24)$$

where v is the measured wind speed and V_c, V_f, V_r the cut-in speed, cut-off speed and the rated speed of wind turbine respectively, and $f(v)$ is a (Weibull, Rayleigh) probability distribution function. Since the measured speeds are discrete values, Eq. (24) can be transformed from integral to sum as shown in Eq. (25).

$$CF = \frac{1}{V_r^3} \sum_{v=V_c}^{V_r} v^3 f(v) + \sum_{v=V_r}^{V_f} f(v) \quad (25)$$

Given the value of the capacity factor, the estimated value that a turbine with rated power $P_r[kw]$ can generate during a specified period of time ΔT [number of hours of interval] can be calculated according to the following relationship as given by Eq. (26).

$$E_{generated} = CF \times P_r[kw] \times \Delta T \quad (26)$$

4 Result and Discussion

4.1 Monthly and Annual Mean Wind Speed

The arithmetic Statistics of the speeds measured at a height of 3 m are shown in Tab. 3, and we note that the data for the years 2011 and 2015 are incomplete. Therefore, the monthly statistical values were calculated from the available measurements in each year, while the annual statistics were calculated from the total sum of the data block values of 1221 values, and the last three columns in the table will be focused. Fig. 1 shows the average wind speed in the study area for five years (2011 to 2015) at a height of 3 m for a period of twelve months.

It is evident from Fig. 1 and the last three columns of Tab. 2 that the average wind speed values are large and southerly over a period of 8 continuous months starting in October and ending in May of the following year, which are the months of autumn, winter and spring. In the summer months of June, July and August, the values of average wind speed are low and northwesterly. This facilitates a mechanism for selecting the type and destination of the wind turbine.

In this study, the cubic statistics of the measured wind speed were also calculated using Eq. (15) in order to calculate the wind power density that is directly proportional to the cube of the wind speed and not with the speed itself. Tab. 3 shows the monthly and yearly arithmetic

and cubic statistics, where the \bar{v}_{Cub} will be used later to calculate the monthly and yearly power density and compare it to the power density expected from the probability distribution functions using Eqs. (19)–(21) above.

Table 3: The monthly and yearly arithmetic and cubic statistics at $h = 3\text{m}$

Statistics	Arithmetic statistics		Cubic statistics
	\bar{v}	σ	
Month	\bar{v}	σ	\bar{v}_{Cub}
Jan	5.17	2.20	5.95
Feb	6.24	2.83	7.46
Mar	6.05	2.23	6.77
Apr	4.87	1.99	5.54
May	3.71	1.62	4.29
Jun	2.18	1.53	3.21
Jul	2.16	1.31	2.84
Aug	1.98	1.29	2.78
Sep	2.45	1.11	2.92
Oct	4.00	1.77	4.65
Nov	4.85	1.60	5.32
Dec	4.97	1.71	5.49
Annual	4.11	2.35	5.19

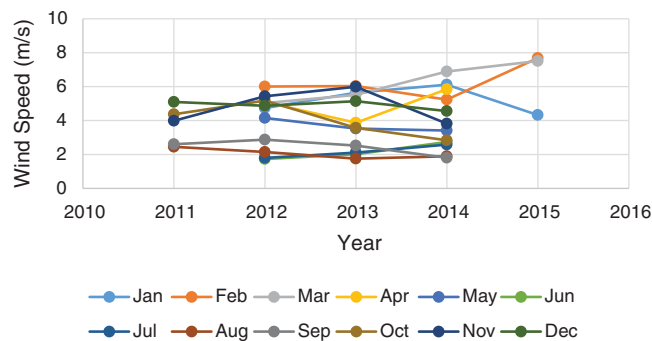


Figure 1: Average wind speed in OYMK for five years (2011 to 2015) at $h = 3\text{ m}$

4.2 Wind Speed Distribution

Weibull and Rayleigh’s parameters are computed for monthly and yearly arithmetic statistics using Eqs. (3), (4), and (7) above. Tab. 4 shows the values of these parameters. Figs. 2 and 3 show the probability and cumulative distribution of the actual wind speed, and the probability and cumulative distribution of Weibull and Rayleigh’s functions based on their parameters calculated based on arithmetic statistics. it is noted from these figures that these probability and cumulative distributions of the Weibull function are more closely related to the probability and cumulative distribution of the actual values.

Table 4: The monthly and yearly arithmetic and cubic statistics at $h = 3$ m

Statistics	Arithmetic statistics		Weibull		Rayleigh	Cubic statistics
	\bar{v}	σ	c	k	c_R	\bar{v}_{Cub}
Jan	5.17	2.20	5.82	2.53	6.57	5.95
Feb	6.24	2.83	7.04	2.36	7.94	7.46
Mar	6.05	2.23	6.78	2.96	7.65	6.77
Apr	4.87	1.99	5.48	2.65	6.18	5.54
May	3.71	1.62	4.18	2.47	4.72	4.29
Jun	2.18	1.53	2.40	1.47	2.71	3.21
Jul	2.16	1.31	2.43	1.73	2.74	2.84
Aug	1.98	1.29	2.21	1.59	2.49	2.78
Sep	2.45	1.11	2.77	2.36	3.12	2.92
Oct	4.00	1.77	4.51	2.42	5.09	4.65
Nov	4.85	1.60	5.41	3.33	6.10	5.32
Dec	4.97	1.71	5.55	3.18	6.27	5.49
Annual	4.11	2.35	4.63	1.86	5.22	5.27

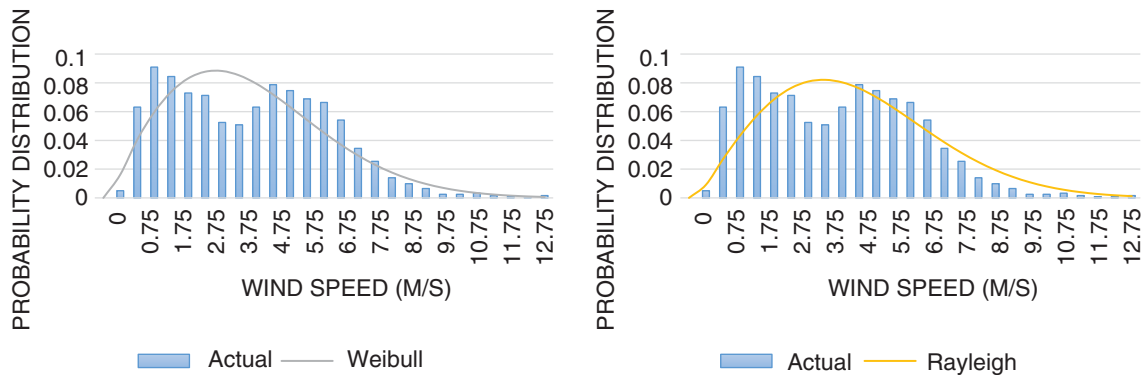


Figure 2: Probability distribution of the actual with (a) Weibull function (b) Rayleigh function

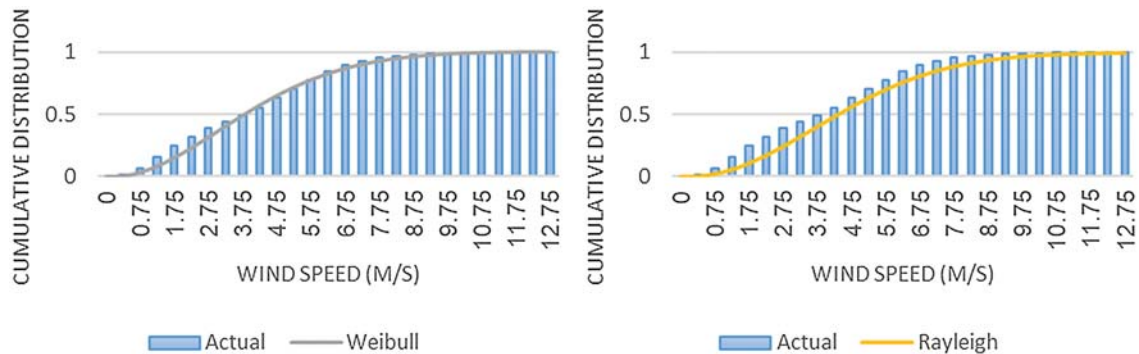


Figure 3: Cumulative distribution of the actual with (a) Weibull function (b) Rayleigh function

4.3 Wind Resource Assessment

The evaluation of wind resources includes the calculation of the power density generated by the wind at the study site by Eq. (19) above, after calculating the statistics at different heights with Eq. (22) above, and includes the evaluation of the power density using the Weibull and Rayleigh probability distribution functions according to Eqs. (20) and (21) above. In evaluating wind resources also, the wind rose analysis is very important to calculate wind power density.

4.3.1 Evaluation of Power Density

The wind power density is directly proportional to the cube of the wind speed according to the relation 19, so the process of calculating the power density from arithmetic statistics for measurements of the wind speed \bar{v} is wrong. The correct procedure is to calculate the power density from cubic statistics for measurements of wind speed \bar{v}_{Cub} according to Eq. (15) above.

If \bar{v}_{Cub} was not previously calculated and only \bar{v} is available, then the power density can be evaluated using the Weibull and Rayleigh probability functions using Eqs. (20) and (21) above as shown in Tab. 5.

Table 5: Calculation and evaluation of power density at h= 3m

Statistics Month	Arithmetic statistics		Cubic statistics		Weibull		Rayleigh	
	\bar{v}	$P_{DA} = 0.5\rho\bar{v}^3$	\bar{v}_{Cub}	P_{DCub}	\bar{v}_w	P_{Dw}	\bar{v}_R	P_{DR}
Jan	5.17	84.64	5.95	129.02	6.00	132.02	6.41	161.65
Feb	6.24	148.82	7.46	254.29	7.37	245.12	7.74	284.22
Mar	6.05	135.64	6.77	190.05	6.79	192.00	7.51	259.04
Apr	4.87	70.74	5.54	104.14	5.59	107.17	6.04	135.11
May	3.71	31.28	4.29	48.36	4.33	49.68	4.60	59.74
Jun	2.18	6.35	3.21	20.26	3.06	17.59	2.70	12.12
Jul	2.16	6.17	2.84	14.03	2.83	13.95	2.68	11.79
Aug	1.98	4.75	2.78	13.16	2.69	11.94	2.46	9.08
Sep	2.45	9.01	2.92	15.25	2.90	14.93	3.04	17.20
Oct	4.00	39.20	4.65	61.58	4.69	63.29	4.96	74.87
Nov	4.85	69.88	5.32	92.22	5.34	93.31	6.02	133.45
Dec	4.97	75.19	5.49	101.35	5.51	102.34	6.17	143.61
Annual	4.11	42.52	5.27	89.65	5.23	87.76	5.10	81.21

Fig. 4 shows a monthly, annually, clear comparative of Weibull speed \bar{v}_w , Rayleigh speed \bar{v}_R and the cube root of mean wind speeds \bar{v}_{Cub} . It is noticeable that the Weibull speed \bar{v}_w approaches the cube root of mean wind speeds \bar{v}_{Cub} compared to the Rayleigh speed \bar{v}_R .

Fig. 5 also shows the other comparative of the actual power density P_{DCub} and the estimated power density of the Weibull distribution P_{Dw} and Rayleigh distribution P_{DR} . It is noticeable that the estimated power density of the Weibull distribution P_{Dw} is close to the actual power density compared to the Rayleigh distribution, that mean the Weibull speed \bar{v}_w is adequate to estimate the power density if \bar{v}_{Cub} wasn't available and only \bar{v} is available.

For further verification, the performance analysis methods are computed according to Eqs. (16)–(18) above as shown in Tab. 6.

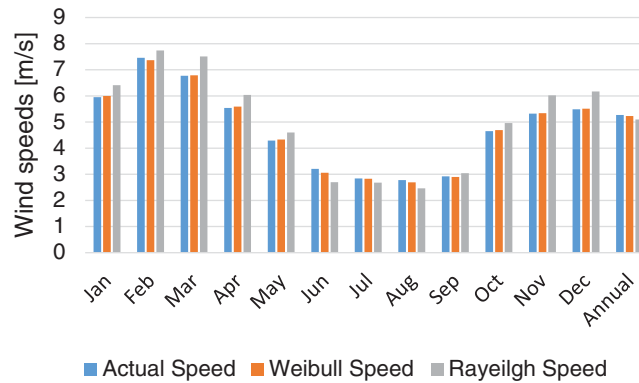


Figure 4: Weibull, Rayleigh, and Cube root of mean wind speeds at h = 3 m

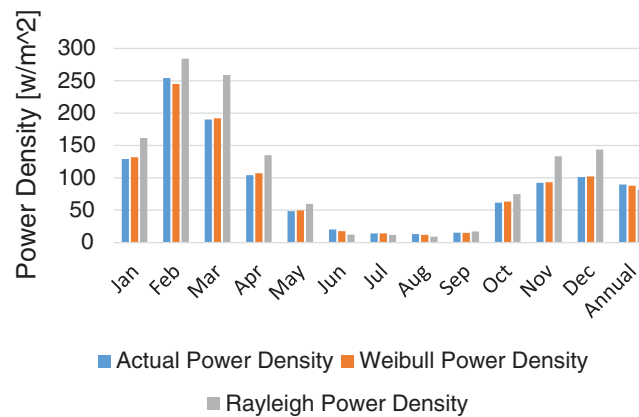


Figure 5: Weibull, Rayleigh, and actual power density at h = 3 m

Table 6: Results of performance analysis methods

Performance analysis method	Min value	Max. value	Optimum value	Weibull	Rayleigh
R^2	0	1	$0 \rightarrow 1$	0.9984	0.9148
RMSE	0	1	$0 \leftarrow 1$	0.0632	0.4680
COE	0	∞	$0 \rightarrow 1 \leftarrow \infty$	1.0280	1.3322

Tab. 6 shows the result of using three performance analysis methods to compare the performance of the Weibull and Rayleigh probability distribution functions in calculating wind power density based on the arithmetic statistics of wind speed \bar{v} only. These methods are the coefficient of determination (R^2), and when its value reaches one, the function used was better. The second method was Root mean square error (RMSE), and when its value is close to zero, the function used was better, and the third method of efficiency coefficient (COE), Which when its value is close to an integer one, whether it comes from a lower level or a higher level, the better the function used. It is noted that the Weibull distribution gives the best values for these three methods, so this distribution can be considered as a good solution for finding power density from the arithmetic statistics of wind speed v only.

Since the height of the tower in the wind turbine ranges between 30 and 100 m, we should use Hellman’s exponential law (Eq. (22) above) to calculate the annual power density at these heights as shown in Tab. 7. Fig. 6 illustrate the conversion results as follows considering $\alpha = 0.19$.

Table 7: Power density at 3, 30, 50 and 100 m

Statistics	Arith.	Cubic		Weibull		Rayleigh	
Height (m)	\bar{v}	\bar{v}_{Cub}	P_{DCub}	\bar{v}_w	P_{Dw}	\bar{v}_R	P_{DR}
3	4.11	5.27	89.65	5.23	87.76	5.1	81.21
30	6.37	8.16	333.1	8.10	326.1	7.90	301.7
50	7.02	8.99	445.7	8.93	436.3	8.70	403.7
100	8.01	10.3	661.6	10.18	647.7	9.93	599.3

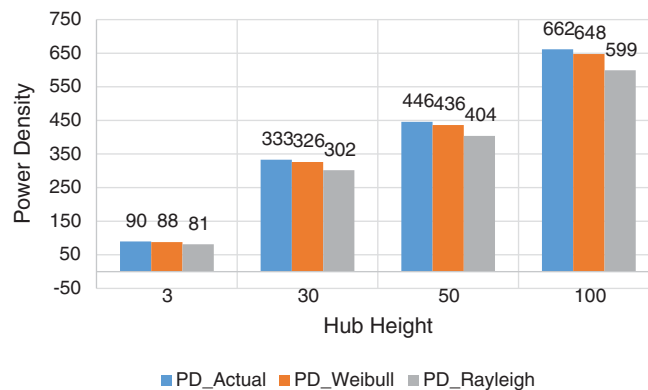


Figure 6: Power density at 3, 30, 50 and 100 m

4.3.2 Wind Rose Analysis

Wind direction analysis is very important to calculate wind power density. In previous studies, the wind rose diagram was very popular to know the direction of the wind, and from this analysis, it is possible to know the direction in which the maximum wind energy can be generated. Returning to Tab. 2, we notice that the prevailing direction of the wind is the south direction. Fig. 7 shows the wind rose diagram. For the study site at a height of 3 m. Tab. 8 shows the exact values for this scheme. The chart and table were extracted from a university site where the wind rose diagram was divided into sections of 30 degrees. The wind direction did not change with altitude.

It is evident from Fig. 7 and Tab. 8 that the winds blow most days of the year as the rate of calm in wind speed reached 6.17%, which equates to only 23 days per year, and it is noted that the direction of the south is the best direction that the turbine can be directed to. The speed of the southern winds reached 62.39% of the annual average of wind speeds, as these winds blow on 227 days out of 365 days a year, which are mostly in eight months of the year (from October to May next year).

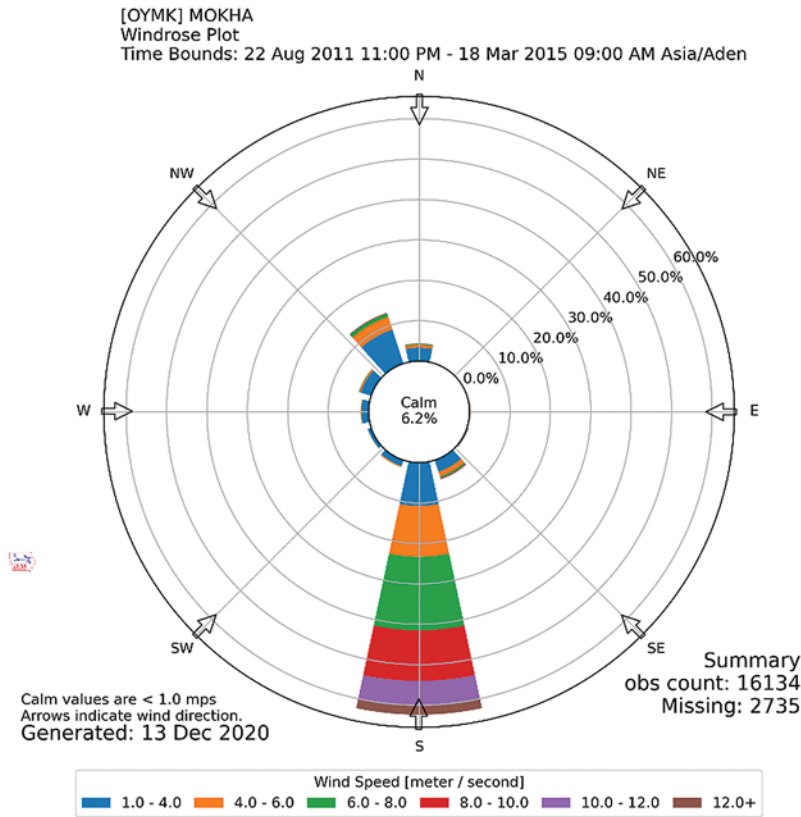


Figure 7: The wind rose diagram

Table 8: The exact values for wind rose at h = 3 m

Direction	Wind speed (m/s) at h = 3 m							Total Percent (%)	Days/year	\bar{v} m/s
	Clam (%)	1-3.9 (%)	4-5.9 (%)	6-7.9 (%)	8-9.9 (%)	10-11.9 (%)	12.0+ (%)			
345°-14° N	6.17%	3.344	0.732	0.224	0.067	0.007	0.007	4.38	15.99	3.23
15°-44° N/NE	22.53 days	0.105	0.052	0.015	0.015	0.007	0	0.194	0.71	4.28
45°-74° NE/E		0.015	0	0	0	0	0	0.015	0.05	2.45
75°-104° E		0.149	0.075	0.022	0.022	0.007	0.03	0.305	1.11	4.99
105°-134° E/SE		0.269	0.037	0.037	0.045	0.022	0	0.41	1.5	4.25
135°-164° SE/S		3.038	1.232	0.478	0.164	0.06	0.007	4.98	18.17	3.83
165°-194° S		10.742	12.586	18.16	12.56	6.151	2.187	62.39	227.7	5.27
195°-224° SW/S		1.515	0.269	0.022	0	0	0	1.81	6.59	2.88
225°-254° SW/W		0.866	0.067	0	0	0	0	0.933	3.41	2.63
255°-284° W	1.784	0.127	0.037	0.007	0.015	0.007	1.98	7.22	2.82	
285°-314° NW/W	2.695	0.426	0.09	0.015	0	0	3.23	11.77	2.94	
315°-344° NW/N	8.853	3.307	0.911	0.134	0.007	0.007	13.22	48.25	3.46	

Note: S = South, N = North, E = East, W = West, SE = Southeast, ES = Southwest, NW = Northwest, and NE = Northeast.

The average value of the speed of the south wind during this period is equal to 5.27 m/s at a height of 3 m, so the direction of the south is the direction chosen in this study.

4.4 Choosing the Appropriate Turbine for the Study Site

The proposed turbine capacity is a turbine with a capacity of 3.45 Mw, as one turbine is sufficient to meet the basic needs of 1452 homes in Mokha region, and since the height of the tower is 100 m, we should use Hellman's exponential law (Eq. (22) above) to calculate the average wind speed at this height as shown in Tab. 9.

Table 9: The exact values for wind rose in south direction and $h = 100$ m

Direction	Wind speed (m/s) at $h = 100$ m							Total Percent	Days/year	Vm m/s
	Clam	4.8	6.9	13.5	17.4	21.3	23.4+			
165°–194° S	6.17%	10.74%	12.59%	18.16%	12.56%	6.15%	2.19%	62.4%	227.7	10.3

Wind energy is harvested in the turbine between the cut-in speeds and the cut-off, which means that the efficient wind speeds that could be used to generate power fall between these two values. The analysis is based on the cut-in and cut-off speeds of the wind turbine.

The IEC has classified wind turbines into three classes. Tab. 10 shows the characteristics of each class.

In this study, the capacity factor was calculated using Eq. (25). Tab. 10 and Fig. 8 show the values of the capacity factor for each class of turbine at the study site.

It is noticeable that Class 3 turbines have the largest capacity parameter, which makes them the best choice, but there are other criteria that must be met to choose the turbine besides the capacity factor standard.

Table 10: The IEC classified of wind turbines

Generic 3.45 MW	IEC Class 1	IEC Class 2	IEC Class 3
Rated power (kW)	3450	3450	3450
Rated Power Wind speed m/s	13	12	11.5
Cut-in m/s	4	3	3
Cut-out m/s	25	22.5	22.5
Design annual average wind speed at hub height m/s	10	8.5	7.5
Rotor diameter (m)	112	126	136
Power Density P_D (w/m^2)	350.2	276.7	237.2
Hub heights (m)	100	100	100
Mean turbulence intensity at 15 m/s I_{15}	18%	16%	12%
50-year extreme wind speed over 10 min V_{ref} [m/s]	50	42.5	37.5
50-year extreme gust over 3 s $V_{50,gust}$ [m/s]	70	59.5	52.5
Capacity factor CF	0.533	0.625	0.671

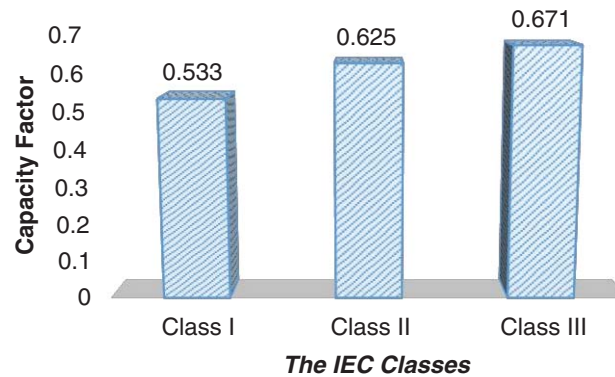


Figure 8: The capacity factor of the IEC classes of wind turbines

The other criteria was the mean turbulence intensity I_{15} that standard for the turbine at 15 m/s I_{15} , the maximum wind speed standard for 50 years is more than 10 min V_{ref} and the standard for a severe storm for 50 years is more than 3 s V_{50} .

It is noted the class I turbine have the top values for those three criteria, and because the study site is a site exposed to storms, so the Generic 3.45 MW-IEC Class 1 turbine is preferred for this site.

To calculate the amount of energy a class 1 turbine generates during the year if it is directed to the south, Eq. (26) shown above can be used and thus Tab. 11 shows the amount of energy in megawatt hours.

In order to calculate the amount of energy a Class 1 turbine generates during the year, if it is directed to the south during 227 days, Eq. (26) can be used thus Tab. 11 shows the amount of energy in MWh of Mokha (1447 dwellings). The daily share of each home of this estimated energy equals 19 KWh, which is enough to cover the basic home loads.

Table 11: The estimated energy by class I turbine

Generic 3.45 MW Class I	Annual MWh	Daily KWh
Annual Energy in MOKHA MWh	10,021	27,838
Total Energy to each household	6.93	19

5 Conclusion

The study site is exposed to high-speed winds, especially the southern winds, which have an average speed of 10 m/s at a height of 100 m, which blow from 227 days from the day of the autumn solstice at the end of December until the summer solstice in June of the following year. It has been proved that the estimated power density by the Weibull probability distribution function P_w is very close to the actual power density P_{Cub} as we obtained excellent values for the performance evaluation criteria: $R^2 = 0.9984$, $RMSE = 0.0632$, $COE = 1.028$. Weibull speed \bar{v}_w can be used to assess the power density in the event that a cubic average of wind speed cannot be obtained at locations adjacent to the study site. The capacity factor was calculated for the three classes classified according to IEC, and the values of this parameter were good for all of these

classes with a slight variation. It has been proven that class I turbines are suitable for the study site that is exposed to major storms, since the coefficients of V_{ref} and $V_{50,gust}$ for this class are large compared to others. The annual and daily amount of energy that one class I turbine can generate was evaluated to meet the needs of 1447 houses in the city of Mokha, and the amount of energy likely to provide to each housing is about 19 KWh per day, which is suitable for feeding the basic loads of each house. This study can be expanded to include areas close to Mocha, such as the Dhobab region, and the areas adjacent to the Bab al-Mandab strait, to establish a large wind farm to feed the Taiz governorate. The process of evaluating the potential energy from this turbine to meet the energy need for the Mocha region is imprecise, because this system needs an energy storage system because the wind is only present during 62% of the days of the year. Therefore, in the future, a detailed study of the possibility of integrating this turbine into a hybrid power system with wind energy or with diesel generators can be conducted.

Funding Statement: The author extends his appreciation to the Deanship of Scientific Research at King Khalid University for funding this work under Grant Number (RGP.1/147/42), Received by Fahd N. Al-Wesabi. www.kku.edu.sa.

Conflicts of Interest: The author declares that they have no conflicts of interest to report regarding the present study.

References

- [1] S. Kutty, M. Khan and M. Ahmed, "Wind energy resource assessment for Suva, Fiji, with accurate Weibull parameters," *Energy Exploration & Exploitation*, vol. 37, pp. 1009–1038, 2019.
- [2] L. Paraschiv, S. Paraschiv and I. Ion, "Investigation of wind power density distribution using Rayleigh probability density function," *Energy Procedia*, vol. 157, pp. 1546–1552, 2019.
- [3] A. Liu, Y. Ma, J. Gunawardena, P. Egodawatta, G. Ayoko *et al.*, "Heavy metals transport pathways: The importance of atmospheric pollution contributing to stormwater pollution," *Ecotoxicology and Environmental Safety*, vol. 164, pp. 696–703, 2018.
- [4] A. Alkholidi, "Renewable energy solution for electrical power sector in Yemen," *International Journal of Renewable Energy Research*, vol. 3, pp. 803–811, 2013.
- [5] Y. Li, W. Xiao-Peng, L. Qiu-Sheng and K. Fah, "Assessment of onshore wind energy potential under different geographical climate conditions in China," *Energy*, vol. 152, pp. 498–511, 2018.
- [6] M. Salah, I. Supérieur and S. Ben, "Assessment of wind energy potential and optimal electricity generation in Borj-Cedria," *Renewable and Sustainable Energy Reviews*, vol. 15, pp. 815–820, 2017.
- [7] I. Fyrippis, P. Axaopoulos and G. Panayiotou, "Wind energy potential assessment in Naxos Island, Greece," *Applied Energy*, vol. 87, pp. 577–586, 2017.
- [8] S. Haralambos, G. Mihalakakou and L. Al-Hadhrami, "Wind power potential assessment for seven buoys data collection stations in Aegean Sea using Weibull distribution function," *Journal of Renewable and Sustainable Energy*, vol. 4, pp. 1–17, 2012.
- [9] M. Baseer, J. Meyer, S. Rehman and M. Alam, "Wind power characteristics of seven data collection sites in Jubail, Saudi Arabia using Weibull parameters," *Renewable Energy*, vol. 102, pp. 35–49, 2017.
- [10] M. Almekhlafi, "Justification of the advisability of using solar energy for the example of the Yemen Republic," *Scientific and Technical Journal*, vol. 4, pp. 51–50, 2018.
- [11] A. Rawea and S. Urooj, "Strategies, current status, problems of energy and perspectives of Yemen's renewable energy solutions," *Renewable and Sustainable Energy Reviews*, vol. 82, pp. 1655–1663, 2018.
- [12] M. Al-Buhairi and A. Al-Haydari, "Monthly and seasonal investigation of wind characteristics and assessment of wind energy potential in Al-Mokha, Yemen," *Energy and Power Engineering*, vol. 4, pp. 125–131, 2012.

- [13] M. Al-Buhairi, "Analysis of monthly, seasonal and annual air temperature variability and trends in Taiz city-Republic of Yemen," *Journal of Environmental Protection*, vol. 1, pp. 401–409, 2010.
- [14] M. Al-Buhairi, "A statistical analysis of wind speed data and an assessment of wind energy potential in Taiz-Yemen," *Assiut University Bulletin for Environmental Researches*, vol. 9, pp. 21–33, 2006.
- [15] A. AL-Ashwal, "All renewable energy applications in Yemen are best practice," *ISECO Science and Technology Vision*, vol. 1, pp. 45–50, 2005.
- [16] L. Gabriela, C. Balaceanu and S. Stefan, "Annual air pollution level of major primary pollutants in Greater Area of Zucharest," *Atmospheric Pollution Research*, vol. 6, pp. 824–834, 2015.
- [17] T. Arslan, Y. Murat Bulut and A. Yavuz, "Comparative study of numerical methods for determining Weibull parameters for wind energy potential," *Renewable and Sustainable Energy Reviews*, vol. 40, pp. 820–825, 2014.
- [18] A. Al Shamma'a, K. Addoweesh and A. Eltamaly, "Optimum wind turbine site matching for three locations in Saudi Arabia," *Advanced Materials Research*, vol. 347, pp. 2130–2139, 2011.
- [19] T. Chang, "Estimation of wind energy potential using different probability density functions," *Applied Energy*, vol. 88, pp. 1848–1856, 2011.
- [20] UNDP, Policy Note, *Prospects of Solar Energy in Yemen*. Sana'a, Yemen: UNDP, 2014.
- [21] M. Hadwan and A. Alkholidi, "Solar power energy solutions for Yemeni rural villages and desert communities," *Renewable and Sustainable Energy Reviews*, vol. 57, pp. 838–849, 2016.
- [22] M. Almekhlafi, "Justification of the advisability of using solar energy for the example of the Yemen Republic," *Scientific and Technical Journal—Technogenic and Ecological Safety*, vol. 42, no. 2, pp. 41–50, 2018.
- [23] Guide to renewable energy and energy efficiency in the Arab states, league of Arab states, 2013.
- [24] N. Arreyndip, E. Joseph and A. David, "Wind energy potential assessment of Cameroon's coastal regions for the installation of an onshore wind farm," *Heliyon*, vol. 2, no. 11, pp. 1–19, 2016.